

Ab initio description of spin pumps and spin sinks in magnetic double layers with in-plane coupling

P. Weinberger

Center for Computational Nanoscience, Seilerstätte 10/21, A-1010 Vienna, Austria

(Received 6 September 2010; revised manuscript received 22 November 2010; published 28 March 2011)

For magnetic double layers separated by a nonmagnetic metallic spacer the precession of the magnetization in only one magnetic slab (“spin pump”) and in both of them (“spin sink”) is described using the fully relativistic spin-polarized screened Korringa-Kohn-Rostocker method. It is found that both semiaxes of the ellipses that form the base planes of precessional cones can be identified with particular anisotropy energies. Slopes along particular paths of the obtained free energy hypersurfaces are then used to estimate in terms of the Landau-Lifshitz-Gilbert equation the minimal times to move from a chosen initial state to a particular final state. Furthermore, fully relativistic spin-polarized calculations by means of the Kubo equation of the corresponding zz -like elements of the conductivity tensor show that the current along the surface normal is bigger for “spin pumps” than for “spin sinks.” For moderately small external fields the time scale for the individual processes is in the femtoregime.

DOI: 10.1103/PhysRevB.83.094428

PACS number(s): 75.70.Cn, 75.70.Ak

I. INTRODUCTION

Very recently ferromagnetic resonance (FMR) and other experimental techniques such as the depth-resolved Kerr effect (TRMOKE) were used^{1,2} to study the magnetization dynamics and electric properties of magnetic double layers $\text{Au}_{12}\text{Fe}_{12}\text{Ag}_n\text{Fe}_{16}$ with $n = 5, 20, 100, 300, 500, 1500$ (in monolayers) grown on a GaAs(100) substrate. The interesting idea behind these experiments was to study the interaction between “spin pumps” and “spin sinks,” namely a change in electric properties when the magnetization precesses only in one of the magnetic slabs (“spin pump”) with respect to a precession in both (“spin sink”). To follow this idea theoretically on an *ab initio* scale implies first to describe the precession of the magnetization in one and in both magnetic slabs on an appropriate quantum mechanical level, then to evaluate the corresponding electric properties, and finally to estimate the time scales for “spin pump” and “spin sink” processes. For this purpose the system $\text{Au}_{12}\text{Fe}_{12}\text{Ag}_5\text{Fe}_{16}/\text{Vac}$ in which the rather thick Au cap is considered as a semi-infinite system³ and the GaAs substrate is replaced by a vacuum barrier was chosen, since due to the small spacer thickness sufficiently large effects can be expected. In particular, the following systems were investigated,

$$\text{Au}(100)/\underbrace{\text{Au}_{12}\text{Fe}_{12}\text{Ag}_2}_{\text{slab 1: } \Theta_1, \Phi_1} \underbrace{\text{AgAg}_2\text{Fe}_{16}\text{Vac}_3}_{\text{slab 2: } \Theta_2, \Phi_2} / \text{Vac}, \quad (1)$$

in which in the left magnetic slab a uniform orientation of the magnetization is characterized by the angles Θ_1 and Φ_1 , and in the right magnetic slab by Θ_2 and Φ_2 . The angles Θ_1 and Θ_2 refer to rotations around the respective in-plane y axes, Φ_1 and Φ_2 around the z axis (parallel to the surface normal) (see Fig. 1), in which it is assumed that the orientations of the magnetization in the two slabs are aligned either parallel or antiparallel to the in-plane x axis.

II. COMPUTATIONAL ASPECTS

All *ab initio* electronic structure calculations were performed at the experimental lattice constant of Au in terms of the spin-polarized (fully) relativistic screened Korringa-Kohn-Rostoker method.⁴ The free energies in Eq. (4) are

evaluated (at zero temperature) in terms of the magnetic force theorem, the electric transport properties by means of the fully relativistic Kubo-Greenwood equation.⁵ In all calculations a maximum angular quantum number of two,⁴ the density functional parametrization of Ref. 6, and the atomic sphere approximation (ASA)⁴ were used.

It should be noted that by using a fully relativistic spin-polarized approach in the context of density functional theory (DFT) the corresponding Kohn-Sham Hamiltonian is given^{4,5} by

$$H(\vec{r}) = c\vec{\alpha} \cdot \vec{p} + \beta mc^2 + V^{\text{eff}}(\vec{r})I_4 + \beta \vec{\Sigma} \cdot \vec{B}^{\text{eff}}(\vec{r}), \quad (2)$$

where

$$\vec{\alpha} = \begin{pmatrix} 0 & \vec{\sigma} \\ \vec{\sigma} & 0 \end{pmatrix}, \quad \beta = \begin{pmatrix} I_2 & 0 \\ 0 & -I_2 \end{pmatrix}, \quad \vec{\Sigma} = \begin{pmatrix} \vec{\sigma} & 0 \\ 0 & \vec{\sigma} \end{pmatrix}, \quad (3)$$

I_m is an m -dimensional unit matrix, $\vec{\sigma} = (\sigma_x, \sigma_y, \sigma_z)$ a formal vector consisting of the usual Pauli spin matrices, and, according to DFT, $V^{\text{eff}}(\vec{r})$ and $\vec{B}^{\text{eff}}(\vec{r})$ refer to the effective potential and exchange field, respectively. Any rotation of this Hamiltonian comprises not only a transformation in coordinate space, but also of the occurring Pauli matrices.⁷ By considering, for example, the last term in Eq. (2) it is easy to show^{4,5} that a transformation in spin space (i.e., of $\vec{\sigma}$) induces a transformation of the orientation of the exchange field $\vec{B}^{\text{eff}}(\vec{r})$, which of course is a classical vector. If, therefore, in the following mainly the term “orientation of the magnetization” is used, in fact a quantum mechanically correct description of the transformation properties of the spin operator $\vec{\Sigma}$ in Eq. (3) applies.

III. FREE ENERGY HYPERSURFACES

According to the specifications in (1) the free energy is given by

$$\begin{aligned} E(\Theta_1, \Phi_1; \Theta_2, \Phi_2) &= E_b(\Theta_1, \Phi_1; \Theta_2, \Phi_2) - E_b(\Theta_1^0, \Phi_1^0; \Theta_2^0, \Phi_2^0) \\ &= \sum_{p=1}^N E_p(\Theta_1, \Phi_1; \Theta_2, \Phi_2), \end{aligned} \quad (4)$$

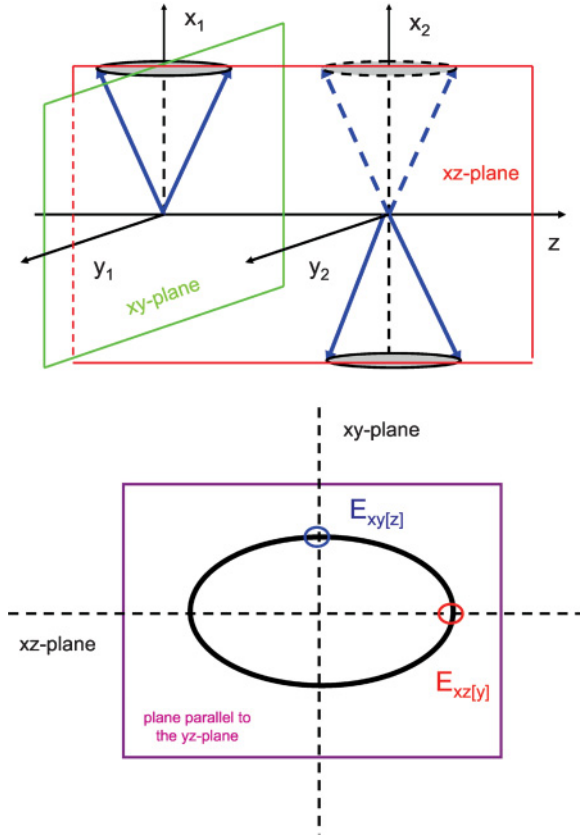


FIG. 1. (Color online) (Top) Perspective view of the precession of the magnetization in both magnetic slabs, that is, considering a typical “spin sink” situation. The cone displayed in dashed lines refers to a parallel alignment. The xy and xz planes indicated specify the cuts through the precession cones. (Bottom) View of the base plane of a precessional cone.

where $E_b(\Theta_1, \Phi_1; \Theta_2, \Phi_2)$ is the grand canonical potential^{4,5} corresponding to a particular choice of these four angles, and $E_b(\Theta_1^0, \Phi_1^0; \Theta_2^0, \Phi_2^0)$ is that of an appropriate reference configuration. In Eq. (4) the $E_p(\Theta_1, \Phi_1; \Theta_2, \Phi_2)$ are the so-called layer-resolved free energies, N being the total number of layers considered. Clearly enough in the case of an in-plane orientation of the magnetization in the two magnetic slabs, depending on the thickness of the spacer (Ag), *a priori* parallel or antiparallel coupling can occur. Therefore, for matters of completeness, in Table I both kinds of coupling are taken into account. In this table $E_{xy[z]}^{xc}(\Phi)$ refers to the interlayer exchange energy, $E_{xy[z]}^a(\Phi)$ to a uniform in-plane anisotropy, $E_{xz[y]}^a(\Theta)$ to a uniform perpendicular anisotropy energy. According to the terms coined in Fig. 1 of Ref. 1 $E_{xz[y]}^{a1}(\Theta)$ and $E_{xy[z]}^{a1}(\Phi)$ have to be associated with “spin pump” energies, while together with $E_{xz[y]}^{a2}(\Theta)$ and $E_{xy[z]}^{a2}(\Phi)$ they correspond to “spin sink” energies.

In a traditional geometrical picture of precession (see the top part of Fig. 1), $E_{xz[y]}^{a1}(\Theta)$ and $E_{xz[y]}^{a2}(\Theta)$ refer to cuts of precessional cones with the xz plane, $E_{xy[z]}^{a1}(\Phi)$ and $E_{xy[z]}^{a2}(\Phi)$ to those with the respective xy planes. Consider like in the bottom part of Fig. 1 the precession of the orientation of the magnetization in only one magnetic slab and a plane (specified by a particular value of Θ) parallel to the yz plane. In this

TABLE I. Definition of various free energies. Θ_1 and Φ_1 specify the (uniform) orientation of the magnetization in the “left” magnetic slab ($\text{Au}_2\text{Fe}_{12}\text{Ag}_2$), Θ_2 and Φ_2 in the right magnetic slab ($\text{Ag}_2\text{Fe}_{16}\text{Vac}_2$) (see also Fig. 1). The superscript xc denotes the interlayer exchange energy, a anisotropy energies, a_1 anisotropy energies if the orientation of the magnetization changes only in the “left” magnetic slab, a_2 refers to anisotropy energies when the orientation changes in both slabs simultaneously. The index denotes the investigated plane and in square brackets is the corresponding rotation axis. For $\Xi = 0$ an alignment parallel to the x axis applies, for $\Xi = 180$ an antiparallel one. The reference magnetic configurations [see Eq. (4)] are compiled in Table II.

Θ_1	Φ_1	Θ_2	Φ_2	E
90	Φ	90	0	$E_{xy[z]}^{xc}(\Phi)$
90	Φ	90	Φ	$E_{xy[z]}^a(\Phi)$
Θ	0	Θ	0	$E_{xz[y]}^a(\Theta)$
Θ	0	90	Ξ	$E_{xz[y]}^{a1}(\Theta)$
Θ	0	Θ	Ξ	$E_{xz[y]}^{a2}(\Theta)$
90	Φ	90	Ξ	$E_{xy[z]}^{a1}(\Phi)$
90	Φ	90	$\Xi - \Phi$	$E_{xy[z]}^{a2}(\Phi)$

plane $E_{xz[y]}^{a1}(\Theta)$ and $E_{xy[z]}^{a1}(\Phi)$ are the major and the minor semiaxis of the ellipse, respectively, that forms the base of the precessional cone.⁸

In the inset of Fig. 2 the interlayer exchange energy $E_{xy[z]}^{xc}(\Phi)$ (see Table I) is displayed for $\text{Au}_{12}\text{Fe}_{12}\text{Ag}_5\text{Fe}_{16}$. As can be seen in this system the two Fe slabs are strongly coupled antiparallel and therefore the antiparallel cases in Table I ($\Xi = 180$) apply [i.e., the reference orientations are in turn $(1,0,0)$ and $(-1,0,0)$] for the two cones displayed in Fig. 1. In Fig. 2, viewed from left to right, $E_{xz[y]}^{a1}(\Theta)$ and $E_{xz[y]}^{a2}(\Theta)$ lead from $(0,0,1)$ to $(1,0,0)$; $E_{xy[z]}^{a1}(\Phi)$ and $E_{xy[z]}^{a2}(\Phi)$ from $(0,1,0)$ to $(1,0,0)$. All curves for “spin-pump” and “spin-sink” energies are “half-parabola”-like shaped, the vertex being when the collinear, antiparallel alignment of the two Fe slabs applies. In the small energy regime ($E \ll 1$ meV) the precession of the orientation of the magnetization forms a conical surface with an almost circular base plane and an aperture of $2(90 - \Theta)$. It should be realized that the energy scale in Fig. 2 is very big indeed and reflects of course the size of the interlayer exchange energy. Because all effects are “big” they show best the difference between a “spin pump” and a “spin sink” situation and of course between major and minor semiaxes.

Since a Fe double layer with a spacer thickness of $n > 5$ monolayers of Ag is also coupled in plane,¹ there is no need to repeat the above analysis for different spacer thicknesses. The only effect to be encountered will be the well-known change between a parallel and an antiparallel alignment (short and perhaps long periods) and the usual decay properties⁹ of $E_{xy[z]}^{xc}(\Phi)$ (and similar ones for all anisotropy energies) when increasing the number of spacer layers.

From Fig. 3 showing the layer-resolved free energies^{4,5} corresponding to $E_{xz[y]}^{a1}(\Theta)$ and $E_{xz[y]}^{a2}(\Theta)$, $\Theta = 30$, it can be seen that all anisotropy effects are confined to the interfaces. In this figure, by going from left to right, the first tip is due to the Au-Fe interface, followed by the two peaks caused by

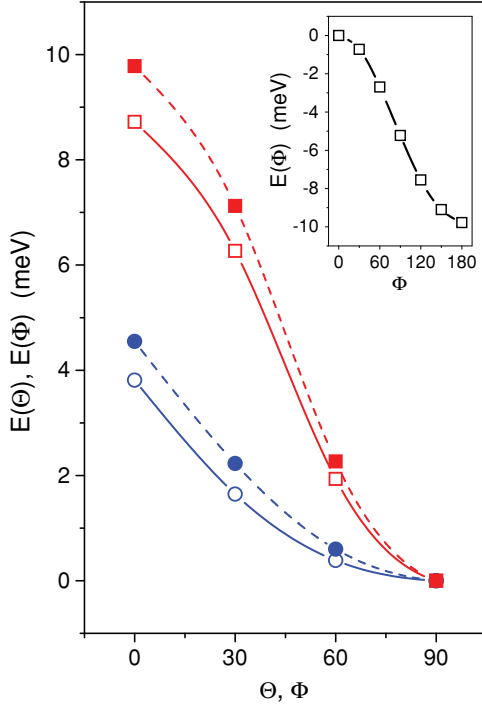


FIG. 2. (Color online) “Spin pump energies” $E_{xz[y]}^{a1}(\Theta)$ (open circles) and $E_{xy[z]}^{a1}(\Phi)$ (solid circles), and “spin sink energies” $E_{xz[y]}^{a2}(\Theta)$ (open squares) and $E_{xy[z]}^{a2}(\Phi)$ (solid squares) in $\text{Au}_{12}\text{Fe}_{12}\text{Ag}_5\text{Fe}_{16}$. The inset shows the interlayer exchange coupling energy $E_{xy[z]}^{xc}(\Phi)$ (see also Tables I and II).

the Fe-Ag interfaces. The small dip to the right is caused by the Fe-substrate interface. Because being confined to the interfaces, interdiffusion effects will be of crucial importance for the actual values of the major and minor semiaxes of the ellipses characterizing precessional cones.¹⁰

IV. ELECTRIC PROPERTIES

Clearly enough not the free energy *per se* is interesting but the changes in the electric properties when going from a “spin pump” to a “spin sink” situation. To answer the question whether a current $j_z(\Theta_1, \Phi_1; \Theta_2, \Phi_2)$ is flowing parallel to the surface normal caused by the difference in these two situations requires one to evaluate in terms of the fully relativistic spin-polarized Kubo equation^{4,5} $\sigma_{zz}(\Theta_1, \Phi_1; \Theta_2, \Phi_2)$, namely the zz elements of the conductivity tensor as a function of those values of $\Theta_1, \Phi_1, \Theta_2$, and Φ_2 that apply to these two situations,

$$j_z(\Theta_1, \Phi_1; \Theta_2, \Phi_2) = \sigma_{zz}(\Theta_1, \Phi_1; \Theta_2, \Phi_2) \mathcal{E}_z = \sum_{p,q} \sigma_{zz}^{pq}(\Theta_1, \Phi_1; \Theta_2, \Phi_2) \mathcal{E}_z^q. \quad (5)$$

Assuming that a uniform electric field \mathcal{E}_z applies in each layer^{4,5} (i.e., $\mathcal{E}_z^q = \mathcal{E}_z, \forall q$), the zz -like conductivity is direct proportional to the current. Consider, for example, $\sigma_{zz}^{(1)}(\Theta) = \sigma_{zz}(\Theta, 0; 90, 180)$ and $\sigma_{zz}^{(2)}(\Theta) = \sigma_{zz}(\Theta, 0; \Theta, 180)$. Then these two conductivities correspond to the “spin-pump” energy $E_{xz[y]}^{a1}(\Theta)$ and the “spin-sink” energy $E_{xz[y]}^{a2}(\Theta)$, respectively. Since from Fig. 2 it is obvious that to each value of $E_{xz[y]}^{a1}(\Theta)$ there exists a value of $E_{xz[y]}^{a2}(\Theta)$ degenerated in energy

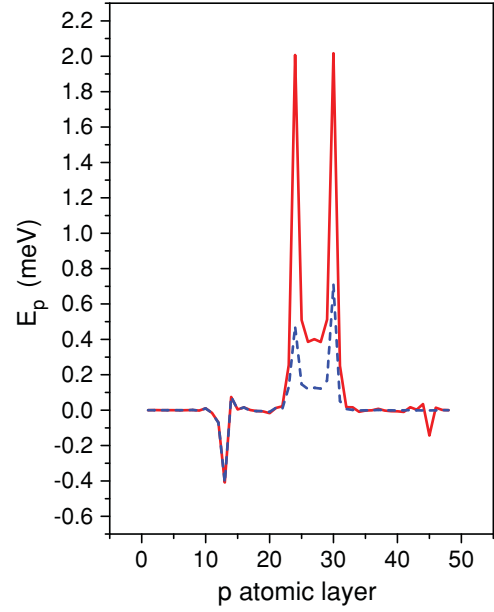


FIG. 3. (Color online) Layer-resolved band energies in $\text{Au}_{12}\text{Fe}_{12}\text{Ag}_5\text{Fe}_{16}$ corresponding to the “spin pump” energy $E_{xz[y]}^{a1}(\Theta)$ (dashed line) and the “spin sink” energy $E_{xz[y]}^{a2}(\Theta)$ (solid line) for $\Theta = 30$.

(i.e., $E_{xz[y]}^{a1}(\Theta) = E_{xz[y]}^{a2}(\Theta) = E$), $\sigma_{zz}^{(1)}(\Theta)$ and $\sigma_{zz}^{(2)}(\Theta)$ have to be displayed as implicit functions of the free energy, for example, as $j_z^{(1)}(E) \sim \sigma_{zz}^{(1)}(E_{xz[y]}^{a1}(\Theta))$. At a given E corresponding “spin pump” and “spin sink” cases are equally probable. Clearly, only as implicit functions of E these two conductivities can be compared to each other. From Fig. 4 it can be seen that at a given energy E (e.g., due to an external magnetic field, finite temperature, etc.) the “spin-pump”-like current is always larger than the “spin-sink”-like one. In this figure the energy range is confined to about 0.5 T (i.e., to energies in principle accessible in experiments). From the inset one can see that in this energy regime the aperture of a precessional (“spin pump”) cone is less than about 10° .

V. ESTIMATE OF TIME SCALES

Although it seems that by now a justification for the terms “spin pump” and “spin sink” have been found in terms of the corresponding electric transport properties, one still has to estimate at least qualitatively the time scales for these processes. Along a particular path on the free energy hypersurface the change of the free energy with respect to the orientation of the magnetization along this path is nothing but the internal field in the Landau-Lifshitz-Gilbert (LLG) equation.¹¹ In using this aspect of a free energy hypersurface the (minimal) time needed to move on such a path from a chosen initial state to a particular final state can therefore easily be obtained.¹¹ In the bottom part of Fig. 4 the times needed to go along the paths corresponding to $E_{xz[y]}^{a1}(\Theta)$ and $E_{xz[y]}^{a2}(\Theta)$, namely $\tau^{(1)}(\Theta)$ and $\tau^{(2)}(\Theta)$ are displayed (again) as implicit functions of the energy, that is, as $\tau^{(1)}(E_{xz[y]}^{a1}(\Theta))$ and $\tau^{(2)}(E_{xz[y]}^{a2}(\Theta))$. As can be seen it takes substantially less time to move along a “sink”-like path than along a “pump”-like path. Considering that a uniform Gilbert damping factor G of

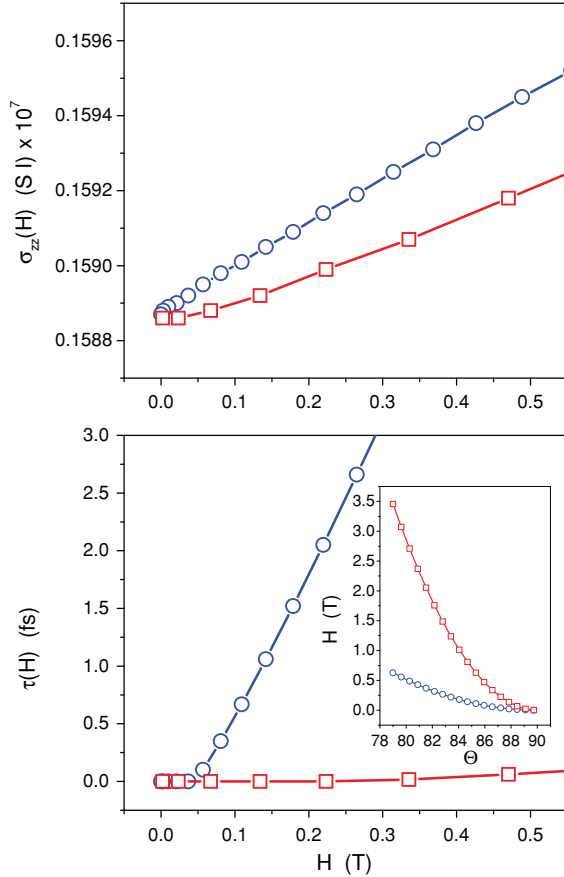


FIG. 4. (Color online) zz -like conductivities $\sigma_{zz}^{(1)}(H)$ and $\sigma_{zz}^{(2)}(H)$ (top) and corresponding switching times $\tau^{(1)}(H)$ and $\tau^{(2)}(H)$ (bottom) corresponding to “spin pump” (squares) and “spin sink” (circles) situations. Shown is the energy range up to about 0.5 T. In the inset $E_{xz[y]}^{a1}(\Theta)$ (circles) and $E_{xz[y]}^{a2}(\Theta)$ (squares) are displayed in this range.

one was used¹¹ to integrate the precessional term in the LLG equation, the times shown in Fig. 4 provide only an estimate of the temporal relation between a “spin-pump” and a “spin-sink” process. It should be noted that to describe the path on the free energy hypersurface that at a given value of E leads from a pump and to a sink situation one has to consider, for example, the condition,

$$\begin{aligned} E &= E_{xz[y]}^{a1}(\Theta) = E(\Theta + \xi, 0; 90 - \mu, 0) \\ &= E_{xz[y]}^{a2}(\Theta') = E(\Theta', 0; \Theta', 0), \end{aligned} \quad (6)$$

in order to scale the minor semiaxes of the ellipses forming the base plane of the precessional cones (see also Tables I and II). In principle, a similar condition, namely $E_{xy[z]}^{a1}(\Theta) = E_{xy[z]}^{a2}(\Theta')$ has to be fulfilled for the major semiaxes. Clearly enough the LLG equation only provides a rough estimate of

TABLE II. Angles specifying the reference magnetic configurations in Eq. (4). For $\Theta_1^0 = \Theta_1^0 = 90$, the cases $\Phi_1^0, \Phi_2^0 = 0$ correspond to $(1, 0, 0)$ (parallel to the in-plane x axis), while $\Phi_2^0 = 180$ corresponds to $(-1, 0, 0)$ (antiparallel to the in-plane x axis).

Θ_1^0	Φ_1^0	Θ_2^0	Φ_2^0	Ξ	E
90	0	90	0	—	$E_{xy[z]}^{xc}(\Phi), E_{xy[z]}^a(\Phi), E_{xz[y]}^a(\Theta)$
90	0	90	0	0	$E_{xz[y]}^{a1}(\Theta), E_{xz[y]}^{a2}(\Theta),$ $E_{xy[z]}^{a1}(\Phi), E_{xy[z]}^{a2}(\Phi)$
90	0	90	180	180	$E_{xz[y]}^{a1}(\Theta), E_{xz[y]}^{a2}(\Theta),$ $E_{xy[z]}^{a1}(\Phi), E_{xy[z]}^{a2}(\Phi)$

the applying time scales for which in principle the time-dependent Dirac equation¹² ought to be used.

VI. CONCLUSION

Within density functional theory the problem of describing the precession of the magnetization reduces to an evaluation of the major and the minor semiaxis of the ellipses⁸ that form the base planes of the precessional cones by taking into account all anisotropy effects in terms of a relativistic approach. It was found that at a given external energy E (external field) the “spin pump” current is always larger than the “spin sink” current. In viewing all data together, one can expect that by supplying a moderately small external field (with a switching on time by at least one order of magnitude larger than τ_1) the system most likely will first move along a path on the free energy hypersurface that leads to a “spin pump” situation, that is, to $E_{xz[y]}^{a1}(\Theta)$ ($\sim E_{xy[z]}^{a1}(\Theta)$), from where it can jump to a degenerated “spin sink” situation, $E_{xz[y]}^{a2}(\Theta)$ ($\sim E_{xy[z]}^{a2}(\Theta)$). In such a process first the conductivity is (slightly) increased, then at $E = E_{xz[y]}^{a1}(\Theta) = E_{xz[y]}^{a2}(\Theta)$ it oscillates along a path as defined in Eq. (6). During switching off of the external field the conductivity falls rapidly back to its initial value, namely that of the collinear ground state, most likely from a “spin sink” situation. In this context it should be recalled that the term “spin current” is very often misleading as implicitly a two-spin current model is assumed. In a relativistic description the use of a polarization operator is needed to define a “current polarization density,”¹² in terms of which then perhaps a time-dependent “spin current” can be interpreted.

Finally, it ought to be pointed out that the approach given clearly does not apply when viewing the magnetization as an average over many-electron ensembles or when having a description in terms of nonequilibrium dynamics in mind. It is entirely based on an “effective” single particle model as provided by density functional theory.

¹O. Mosendz, G. Woltersdorf, B. Kardasz, B. Heinrich, and C. H. Back, *Phys. Rev. B* **79**, 224412 (2009).

²B. Kardasz and B. Heinrich, *Phys. Rev. B* **81**, 094409 (2010).

³The bulk interlayer spacing in bcc Fe, fcc Ag and fcc Au is in turn 2.635, 3.864, and 3.841 a.u.

⁴J. Zablouil, R. Hammerling, L. Szunyogh, and P. Weinberger, *Electron Scattering in Solid Matter* (Springer Berlin Heidelberg New York, 2004).

⁵P. Weinberger, *Magnetic Anisotropies in Nanstructured Matter* (CRC, Boca Raton-London-New York, 2008).

⁶S. H. Vosko, L. Wilk, and M. Nusair, *Can. J. Phys.* **58**, 1200 (1980).

⁷P. Weinberger, *Philos. Mag. B* **75**, 509 (1997).

⁸The canonical implicit equation for an ellipse is of the form $x^2/a^2 + y^2/b^2 = 1$ with a and b being the major and the minor semiaxes, respectively.

⁹See, for example, J. Kudrnovsky, V. Drchal, I. Turek, P. Bruno, and P. Weinberger, *J. Phys. Condens. Matter* **13**, 8539 (2001), and references therein.

¹⁰This can be taken into account using the so-called inhomogeneous coherent potential approximation discussed in Refs. 4, and 5.

¹¹P. Weinberger, A. Vernes, B. L. Gyorffy, and L. Szunyogh, *Phys. Rev. B* **70**, 094401 (2004); A. Vernes, P. Weinberger, and L. Szunyogh, *ibid.* **72**, 0112401 (2005).

¹²A. Vernes, B. L. Gyorffy, and P. Weinberger, *Phys. Rev. B* **76**, 012408 (2007).